The Mach 10 Component of NASA's Hyper-X Ground Test Program

R.J. Bakos* and C.-Y. Tsai†
GASL, Ronkonkoma, NY
and
R.C. Rogers‡ and A.T. Shih§
NASA-Langley Research Center, Hampton, VA

ABSTRACT

The Mach 10 Hyper-X ground test program is described, in which experimental flowpath parametric testing is being done in the HYPULSE facility. This facility has been upgraded for this effort by adding a reflected-shock-tunnel operating mode to access test conditions at Mach 10 and below. A large test section and hypersonic nozzle have been installed to provide full-scale engine test capability and the instrumentation systems have been expanded. A model of the Hyper-X engine flowpath has been built for freejet testing in the shock tunnel at both Mach 7 and 10 flight conditions. The model has over 180 instrumentation ports, a pitot rake mountable at the engine inlet or exit, and optical windows for visualization of the isolator, combustor, and nozzle. Testing in HYPULSE has been completed at Mach 7 conditions to provide a link between pulse facility data and the large Hyper-X performance database that is being accumulated in long-duration facilities. Comparisons of Mach 7 data with computational predictions and with data recently acquired for an identical flowpath being tested in the NASA 8-foot High Temperature Tunnel are presented.

INTRODUCTION

Hyper-X is NASA's focused hypersonic technology program that will move hypersonic, air-breathing vehicle technology from the laboratory to flight. In this program, three autonomously controlled research vehicles will be flown at speeds up to Mach 10. Experimental support to the scramjet engine flowpath development for the Mach 10 flight is being provided by the NASA Hypersonic Pulse Facility, HYPULSE. Although there exists a large and significant database of scramjet engine performance and operation in the flight Mach 4 to 7 range, little data is available at Mach 10 (or above) except for some tests conducted during the NASP program as described in references [1] and [2]. Reviews of the scramjet data and test experience at NASA Langley are provided in references [3] and [4]. Additional details of the Mach 7 Hyper-X ground tests, test facilities, and the relationship to flight testing are provided in references [5] and [6].

To support Hyper-X, the NASA-HYPULSE shock tunnel located at and operated by GASL has been upgraded to include a detonation driven reflected-shock tunnel (RST) operating mode with access to test conditions simulating Mach 7 and 10 flight speeds. The upgraded facility has a test chamber that allows testing of a scramjet engine of the same scale as conventional blow-down test facilities, such as the Langley Arc-Heated Scramjet Test Facility (AHSTF) (see ref. [7]). More information about the operation of HYPULSE is in references [8], [9], [10], and [11].

Developmental testing of the Mach 10 engine flowpath will be done entirely in HYPULSE. In order to provide a benchmark for the Mach 10 data and traceability to the large database and test experience at Mach 7, the Mach 7 Hyper-X flowpath was tested first. A test model of this flowpath, named the HYPULSE Scramjet Model (HSM) was designed, built and tested in HYPULSE. The model is a truncated, partial-width version of the Hyper-X flowpath, and is a twin of the Hyper-X Experimental Model (HXEM) which is being tested in the Langley 8-Foot High-Temperature Tunnel (Ref. [7]). The HSM and HXEM share instrumentation locations to facilitate data comparisons.

HSM was recently reconfigured to replicate the initial Mach 10 flowpath design and testing is currently underway. These tests will add

*Vice President, Research and Advanced Development, Member
†Principal Scientist, HYPULSE Laboratory Manager, Member
‡Aerospace Research Engineer, Hypersonic Airbreathing Propulsion Branch, Senior Member
§ Aerospace Research Engineer, Hypersonic Airbreathing Propulsion Branch, Member

experimental input to the analytical design of the Mach 10 flowpath.

This paper provides a description of the test facility, test conditions, model hardware and plans for the Mach 10 test program. Model data at the Mach 7 condition is presented both in comparison with computational predictions and with data from the long run-duration 8-Ft HTT.

FACILITY DESCRIPTION AND OPERATION

HYPULSE OPERATION

The recently upgraded HYPULSE facility, shown in Figure 1, supports an RST operating mode to complement the shock-expansion tube/tunnel (SET) mode for which the facility was originally designed and built. This new mode allows flight total enthalpy simulation from Mach 5 to 10 in addition to the Mach 12 to 25 capability of the facility when run in SET mode, as shown in Figure 2. As part of the upgrade, a 19-foot long, 7-foot diameter test section and nominal Mach 6.5 hypersonic nozzle were installed to permit installation and testing of large models.

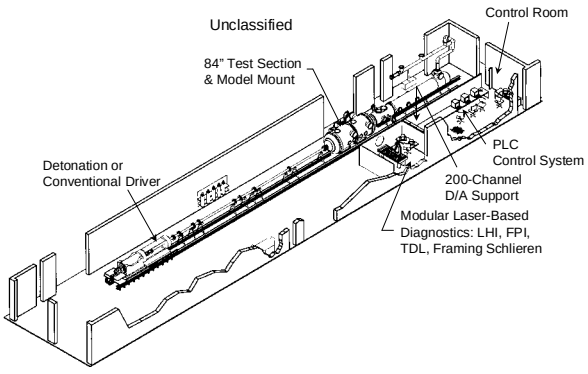

Figure 1.- Upgraded HYPULSE Facility, a Dual-Mode Reflected Shock Tunnel/Shock-Expansion Tunnel

As a shock-heated test facility, the run times of HYPULSE are on the order of milliseconds. To assure that the flow in the model can relax to steady state during the run time, the model size is limited to about 1/3 of the test gas slug length, determined as the product of the steady flow time and the test gas velocity. For the HYPULSE-RST, the model maximum length is about 16 feet at the Mach 7 condition and 6 feet at the Mach 10 condition. An advantage of the short run times is that the model hardware does not get hot, thereby enabling the acquisition of flow visualization data which are not readily obtained in conventional blowdown facilities.

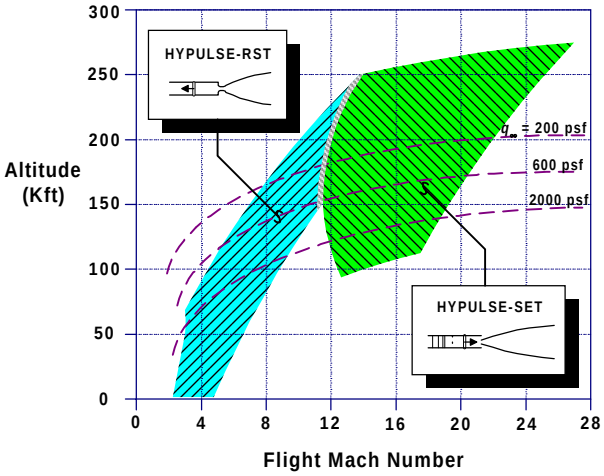

Figure 2.- Simulation Capability of HYPULSE in RST and SET Modes

Test Conditions: A 175:1 area ratio axisymmetric nozzle was designed for HYPULSE to produce local Mach 6.5 exit flow at facility stagnation conditions simulating Mach 10 flight. Details of the design, fabrication, and calibration are given in reference [11]. The nozzle contour was truncated from the fully expanded flow at an axial location near the point where the final characteristic intersected the viscous layer. Measured pitot pressure distributions are shown in Figure 3a for the nozzle at two axial stations downstream of the nozzle exit plane compared with a computational solution from the General Aerodynamics Simulation Program (GASP). These computational solutions were mass averaged over the central 12 inches of the flow to derive the quoted nozzle exit conditions in Table 1.

When the AR175 nozzle is operated "off design" at the stagnation enthalpy corresponding to Mach 7 flight, the nozzle exit Mach number is higher, reaching 7.3 in the core. Wave cancellation is not complete because the ratio of specific heats is different from the design Mach 10 condition. Figure 3b shows that the measured and GASP computed pitot pressure distributions deviate from a constant value at about 5 inches from the axis for the 1-inch station. Further downstream, the flow is more uniform as the uncancelled waves have a chance to propagate further across the flow. The quoted Mach 7 conditions in Table 1 are obtained again by mass averaging the computational solutions. These conditions correspond to a q=500 psf simulation for Hyper-X. Higher dynamic pressure simulations are achieved by increasing the facility stagnation

pressure. Experiments indicate no measurable effect of stagnation pressure on the nozzle exit profiles within the range of interest.

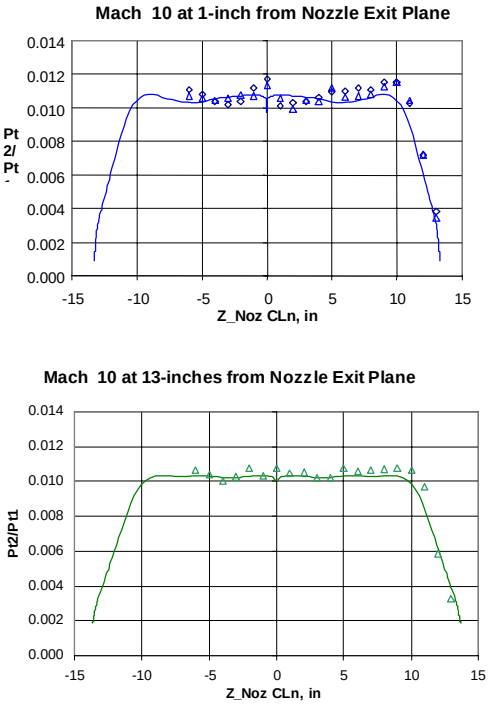

Figure 3a. – Mach 10 measured and computed pitot pressure distributions at two axial stations

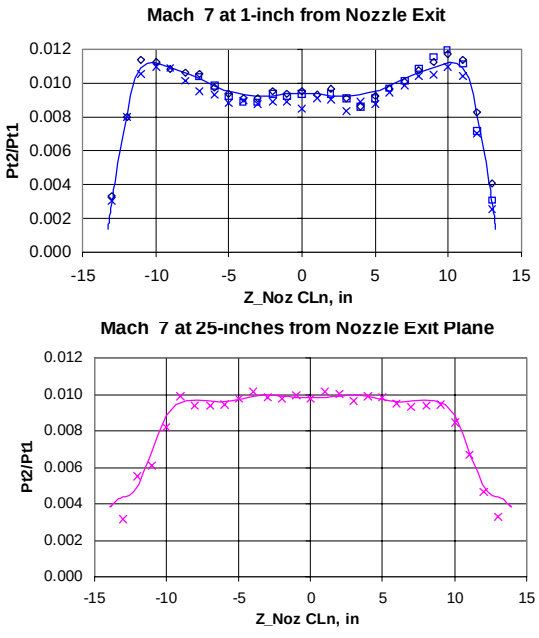

Figure 3b. – Mach 7 measured and computed pitot pressure distributions at two axial stations

DATA AND INSTRUMENTATION INFRASTRUCTURE

HYPULSE is served by a 200-channel data network for high-frequency data recording. The primary data acquisition system is composed of LeCroy 8025 Instrument Mainframes housing 39 4-channel 6810 Waveform Recorders. This assembly acquires up to 156 simultaneous data channels at frequencies to 1 MHz. For static pressure measurements, approximately 200 PCB piezoceramic pressure transducers are available. These instruments have a 500 KHz frequency response and sensitivities ranging from 1 to 100 mV/psi. They are calibrated at GASL and provide a measurement uncertainty of less than 5%. Heat flux gages are manufactured and calibrated at GASL. These are platinum thin-film resistance thermometers painted on MACOR machinable ceramic substrates.

Optical systems for HYPULSE include four-frame high speed schlieren, laser-holographic interferometry (LHI), fuel-plume planar imaging (FPI), and tunable-diode laser path-integrated water vapor (PIW) measurement. The schlieren system is used to visually assess flow establishment and duration through the images acquired at specific times during the flow duration.

ENGINE MODEL

The HYPULSE Scramjet Model (HSM) is a full scale, partial width and length replica of the Hyper-X Research Vehicle (HXRV), as illustrated in Figure 4. The forebody and aftbody (nozzle) are truncated to achieve a model size compatible with the facility limitations. The HSM forebody begins at the start of the HXRV second compression ramp, generally referred to as control point 2. More detail of the simulation conditions is discussed in a later section. The HSM was designed and fabricated in parallel with the HXEM engine that is being tested in the LaRC 8-Ft. HTT.

TEST HARDWARE

Figure 5(a) shows a photograph of the HSM model and Figure 5(b) shows the model installed in the test section, cowl side up. The model design features include a 40% partial width engine section and a fenced forebody that is 2 inches wider (1 inch each side) than the engine inlet to allow for bleed slots to remove the fenced forebody boundary layer. A removable boundary layer trip strip is placed in the forebody to transition the boundary layer before entering the inlet.

Table 1.- Nominal Test Conditions, HYPULSE at M = 7 & 10						
Flight Mach	Stagn. Enthalpy (MJ/kg) [Btu/lb]	Stagn. Press (MPa) [atm]	Nozzle Exit (AR = 175)			
			M	P (kPa) [psia]	T (K) [^{o}R]	V (m/s) [ft/s]
7	2.45 [1050]	5.15 [51]	7.3	0.70 [.101]	208 [374]	2114 [6936]
10	4.6 [1980]	24.0 [237]	6.5	5.02 [.728]	529 [952]	2990 [9810]

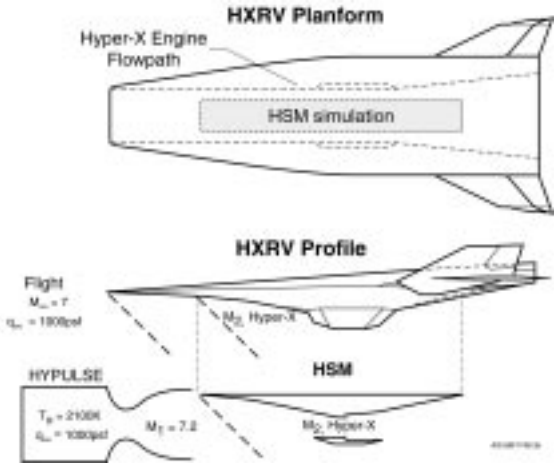

Figure 4.- HSM M7 Simulation Compared to Hyper-X Flight

The injector internal and external geometry are identical to the flight vehicle in truncated width. Joints in the cowl and body-side flow surfaces are readily modified to accommodate the Mach 7 and Mach 10 flowpath configurations with a minimum of hardware rework. The leading edges are replaceable and have radii consistent with the flight vehicle and other full-scale model hardware. The model flowpath surfaces are stainless steel while the sidewalls are aluminum. Two window sets show views of the isolator/combustor and the internal nozzle.

The model was designed to be positioned over a 13.3^{o} variable angle-of-attack range to accommodate both Mach 7 and 10 HXRV simulations. The pivot point is located just below the forebody surface, and at the axial midpoint between the forebody and cowl leading edges. This assures that the captured streamtube originates from the central nozzle core at all angles of attack.

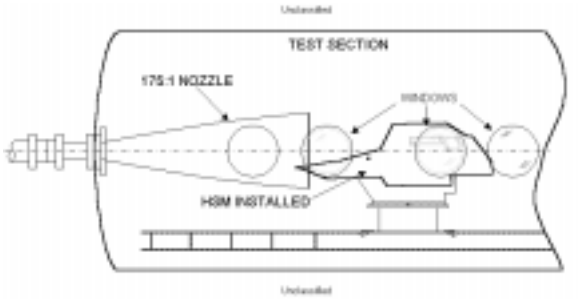

Figure 5(a).- Installation photograph of the HSM installed in HYPULSE with the forebody fences removed for flow visualization

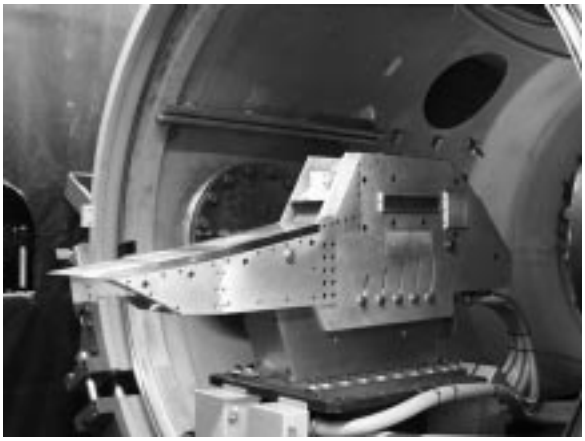

Figure 5(b).- Installation of the HSM in the HYPULSE Test Section

FUEL SYSTEM

Figure 6 shows a typical HSM fuel system schematic. The Ludwieg tube supply provides perfectly steady plenum pressure for 10 ms and is designed to be compatible with mixtures of silane in hydrogen from 0-20% by volume. Independent supplies are used for the body-side and cowl-side plenums.

Each Ludwieg tube and plenum are connected by two Marotta solenoid valves. These have nominal opening times of 2 ms when energized with 150V. The volume downstream of the valves is minimized to achieve steady-state plenum pressure within 10 ms of the valve open trigger as necessary to reliably time the fuel system with the operation of the test facility. A sharp edged orifice meter and pressure transducers are used to measure the fuel flow through each of the valve legs feeding the plenum. For planned implementation of the Fuel Plume Imaging diagnostic, fuel is fed through "seeders" that are designed to entrain a desired amount of micron sized, mono-disperse, silica particles.

INSTRUMENTATION

Surface Data: --Instrumentation layout on the body and cowl side surfaces of the HSM includes 184 pressure and heat flux instrument ports, the majority of which were chosen to be identical to the HXEM model so that point-by-point data comparisons could be made. The PCB transducers are recess mounted behind a .063-inch diameter, .06-inch deep orifice. The platinum thin-film heat flux gages are flush mounted.

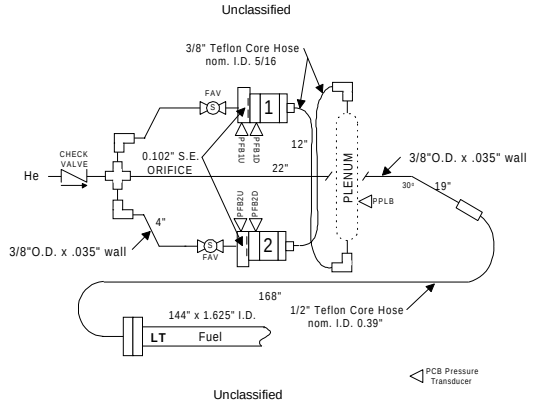

Figure 6.- Typical HSM Fuel System Schematic

Flow Surveys: -- The pitot pressure survey rake used to assess the captured stream tube, and its location relative to the forebody generated shock system, is indicated in the forebody sketch in Figure 7. The pitot rake has 23 probes mounted 0.200 inches apart and its height above the surface is adjustable. Each probe is instrumented with a PCB transducer mounted in the rake body to minimize response time. The shocks formed from the second and third compression ramps cross the rake as indicated. The rake is currently designed for 5 transverse locations and can be mounted at either the cowl leading or trailing edge.

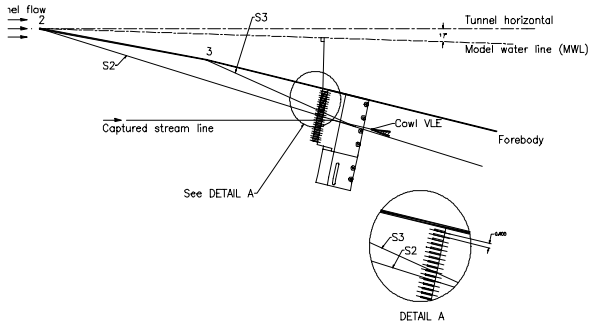

Figure 7.- Location of the Pitot Rake Used to Survey the Captured Airstream

Optical Diagnostics:

There are three major subsystems in the HYPULSE integrated optical system, the high-speed schlieren system, the laser holographic interferometer (LHI), and the fuel plume imaging (FPI) system. Detailed description of the FPI system can be found elsewhere [12]. The schlieren and LHI share a pair of 15-inch diameter field-of-view parabolic mirrors of 90-inch focal length. The two systems also share two main optical tables without conflict, such that conversion from schlieren to interferometric imaging is quickly accomplished by inserting a 2-inch flat mirror in the sending side and removing a 4-inch mirror along the optical path in the receiving side.

The upgraded HYPULSE test section has five different optical window stations to accommodate different nozzle sizes and test article configurations. Multi-station flow visualization capability has also been considered in the system design. The two main optical tables and mounting tables for the parabolic

mirrors all rest on retractable casters so that a move from one axial station to another can be easily made.

The schlieren system uses a high-power AlInGaP LED as the light source, similar to those used by Lu, et al in their Cranz-Schardin camera design [13]. The T-1¾ (5 mm) LED has a narrow viewing angle of 6 degree with a very high luminous intensity of 6500 mcd at a current of 20 mA. The color of the LED emission is red with a peak wavelength of 626 nm and a FWHM of about 15 nm. The LED is powered by a pulsed constant current with a maximum current output of 20 amp. Pulse width can vary from 0.5 to 20 μs with a rise or fall time of less than 100 ns and output current pulses are controlled by input TTL's. The monochromatic nature of the light source allows the implementation of band-pass filters so that the luminosity of the hot gas flow can be filtered.

The schlieren images are captured by four monochrome CCD cameras. The cameras use a high resolution $^{2}/_{3}$" progressive scanning interline transfer CCD imager of 768(H) x 484(V) pixels with cell size of 11.6 μm x 13.6 μm. The cameras can be asynchronously reset with external shutter speed control or internal control at fixed speed range from 1/16000 to 1/125 second (62 μs to 8 ms). Three 50/50 beam splitters are used to uniformly divide the schlieren image into four images, and these are focussed on the CCD imagers by 4 CCTV lenses with focal lengths of 50 mm. For all schlieren images reported here, a fixed shutter speed of 1/16000 was used. The timing of the shutter open dwell for each camera was carefully set to synchronize with the multiple LED emissions, each with a pulse width of 4 μs.

HSM TEST ENTRY DESCRIPTIONS

FIRST ENTRY MACH 7 TESTS

Simulation: The Hyper-X propulsion flowpath for Mach 7 flight conditions is simulated in the HYPULSE RST ground test series in the following manner. The HSM forebody replicates only the second two of the three compression ramps that make up the HXRV forebody. The HYPULSE AR-175 nozzle, when operated at 2100 K (3780 R) stagnation temperature produces an exit Mach number of 7.32. The HSM is placed at a specific rotation angle (angle-of-attack) relative to the nozzle centerline such that a shock wave is formed. The rotation angle was chosen so that the flow Mach number produced behind the shock wave matches that on the second ramp of the HXRV at flight conditions. Conditions on each ramp surface of the forebody were computed using the procedure for one-dimensional isentropic flow of a thermally perfect gas (TPG) as described in reference [14].

The M7 test plan included examining the flowpath operation at q = 500, 1000, and 2000 psf. The q = 500 psf tests provide direct comparison with the database acquired in the LaRC AHSTF (ref [5]). Tests at q = 1000 psf provide information for comparison with flight data and the 8-Ft HTT database, while the high q =2000 psf tests yield data on fuel ignition and flameholding at higher combustor entrance pressures.

Objectives: This first entry was the inaugural of engine testing in the updated HYPULSE RST, hence a critical component of the tests was the development of a scramjet engine test technique, which includes the shakedown of the facility operational procedure, debugging the data acquisition system, assessing the fuel supply system operation, and data processing. Subsequently, the model inlet flow was surveyed to assess engine mass capture. Unfueled and fueled runs were made with pure hydrogen and silane/hydrogen mixtures. Both pure air and pure nitrogen were used as test gases.

SECOND ENTRY, MACH 10 TESTS OF THE M7 FLOWPATH

Simulation: The HSM configured to the M7-Hyper-X flowpath was also tested at Mach 10 conditions to provide facility and model operational experience and data for the Mach 10 HXRV flowpath design process. Conditions on the HSM forebody are computed using the TPG process from facility nozzle plenum (stagnation) conditions of 4100K, which is nominal Mach 10 stagnation temperature, and 250 atm, which is currently the practical upper limit of HYPULSE RST stagnation pressure. Positioning the HSM with its first ramp at a slightly negative angle of attack generates a leading expansion and yields a flight simulation for the Hyper-X at Mach 10 flight conditions. For the P_0 = 250 atm, this simulation corresponds to an approximate flight q = 500 psf. Positioning the HSM with forebody ramp aligned with the tunnel flow, gives a flight simulation for the Hyper-X at a slightly higher angle-of-attack and corresponds to an approximate flight q = 635 psf.

Test Objectives: Descriptions and objectives for the second entry tests included checkout of facility operation at Mach 10 enthalpy and establishment of a practical upper limit of facility stagnation pressure. Calibration surveys of the model mass capture were done to confirm computational predictions. Combustion and mixing runs with corresponding tare (unfueled) runs provided Mach 10 test data for comparison with the analytical design methods used to define the Mach 10 flowpath.

MACH 10 FLOWPATH TEST PLANS

Simulation: The initial design for the Hyper-X Mach 10 flowpath has been completed and the HSM has been reconfigured for testing. Since the time of the design of the HYPULSE Mach 6.5 facility nozzle, the planned angle of attack of the Mach 10 HXRV flight path has changed.

Options to accommodate this change include modifying the existing nozzle or build a new section to achieve an exit Mach above 8. For the first Mach 10 flowpath entry, the existing nozzle will be used resulting in a slight mismatch in Mach number between simulation and flight.

MACH 7 ENTRY RESULTS

Results from the initial entry at of Mach 7 are reviewed and compared to computational solutions and to experiments run in the 8-Ft HTT. Data and analysis from the first Mach 10 entries are currently in preparation.

COMPUTATIONAL SOLUTIONS

Computational solutions of the HSM forebody were run to assess the ability to predict the experimental results and to assist in determining the engine's captured mass flow which is not measured directly. The forebody simulations become the computational starting point for further CFD and engineering analyses of the engine, and good agreement with forebody data lends confidence that the analyses begin with accurate startline conditions. A second requirement for these computations is to assess the mass captured by the engine inlet. This allows fuel flow rates to be set during engine testing such that desired equivalence ratios are achieved. Computations were made of the forebody at inflow conditions near to those for Mach 7 given in Table 1.

Both two and three- dimensional viscous solutions of the HSM forebody were computed using the General Aerodynamic Simulation Program (GASP). The parabolized, thin-layer, Favre-averaged Navier-Stokes equations were solved on a non-orthogonal curvilinear grid. The two-dimensional solution was obtained along the plane of the model centerline. The computational domain extended from the HSM leading edge to the plane of the start of the fuel injectors. The three-dimensional solution was computed for a computational domain extending from the model leading edge to the plane of the cowl leading edge. The code used a thermally perfect gas model for air. Wall temperature was set at a constant 300K to correspond to the conditions in the pulse facility tests. Boundary layer transition on the body side was specified downstream of control point 3 compression ramp. The Baldwin-Lomax turbulent model was used to approximate the turbulent eddy viscosity. Results from the CFD solution were produced in the form of stream pitot pressure contours, wall pressure distributions, and numerically computed schlieren for comparison with their experimental counterparts.

FOREBODY SURFACE AND PITOT PRESSURE

A comparison of the surface pressure distribution on the HSM forebody with computational results is presented in Figure 8a. The CFD predicted pressures were adjusted upward by approximately 9% before plotting in Figure 8a to correct for a difference in the conditions used in the calculation from those reported in Table 1. The latter come from the most recent and accurate nozzle calibration data for the facility. On the first HSM ramp, the comparison between the data and the CFD result is reasonable in the mean, although the presence of weak waves exiting the nozzle is evidenced in the measured pressures. Pressures on the second HSM ramp are somewhat underpredicted by the 3D and especially the 2D solutions, indicating that further refinement of the boundary layer treatment in the computation may be necessary.

Comparisons of measured and predicted pitot pressure profiles just upsteam of the cowl closure, Figure 8b, indicate the predictive capability of the engine capture conditions. These computations are used to determine the engine's captured mass flow.

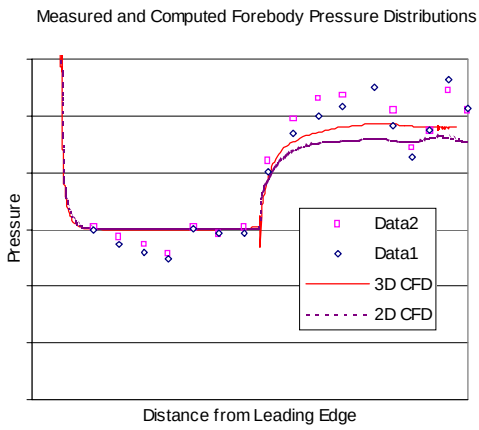

Figure 8(a) – 2-D and 3-D GASP computed static pressure distributions on the HSM forebody.

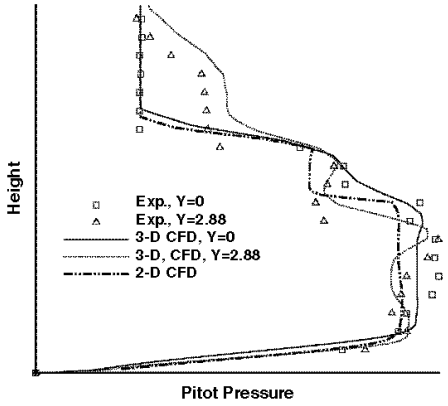

Figure 8(b) - 2-D and 3-D GASP computed Pitot pressure profiles at the end of the HSM forebody.

FOREBODY FLOW VISUALIZATION

Figure 9(a) shows a series of schlieren images on the forebody including the boundary-layer (BL) trip location and the compression corner at control point 3. The series was acquired in two runs with the BL trip installed and covers a test flow time from 1 to 14 ms after shock reflection in the facility nozzle plenum. The BL trips, located just to the left of the image field of view, generate a weak shock wave that has a slope equal to the Mach angle. The boundary layer is visible as a dark band along the forebody.

At 1 ms the starting shock has reached the BL trip location and by 3 ms, shock structure has been established. The flow appears to remain unchanged until about 11 ms when a reduction in contrast occurs indicating arrival of the lower-density helium driver gas. At 14 ms, evidence of helium gas is clear. Detailed review of the pressure histories at several stations along the model indicate that helium begins to affect the data at about 8 ms. Based on these results, for the purposes of extracting steady data from the time traces, an averaging window spanning from 3 to 7 ms was used for all Mach 7 data.

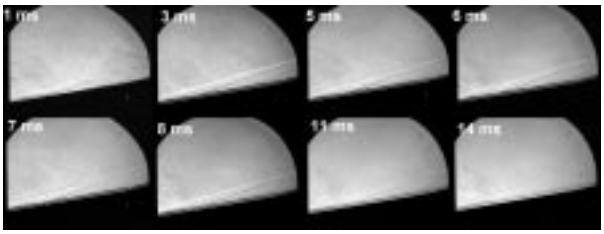

Figure 9(a).- Time resolved schlieren images of flow over the HSM forebody with the BL trip.

Numerical schlieren images, that were generated from the 2D-CFD results, are presented in Figure 12(b), which shows gray-scale filled contours of the transverse gradient of density to approximate the physical parameter observed by the schlieren process. These numerical contours depict a flowfield very similar to the experimental schlieren acquired at 4 ms for a test with the boundary layer trip removed. The light/dark band near the forebody surface is the thermal layer as a result of the 2100K stagnation temperature air flowing over a cold wall (300K). In the light shaded region, the temperature rapidly increases (decreasing density) out to a near stagnation value; in the dark shaded band, the temperature decreases (increasing density) to the stream static value (approximately 400K) at the boundary layer edge.

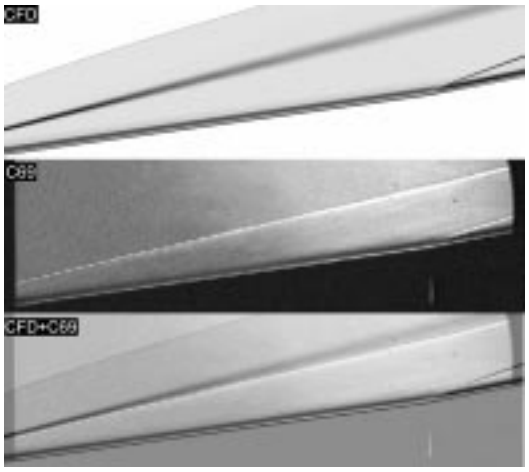

Figure 9(b).- Comparison of numerically generated and experimental schlieren images on the HSM forebody

HSM / HXEM DATA COMPARISON

A preliminary comparison of HSM data to results recently acquired with the HXEM in the 8-Ft HTT has been completed. In both tunnels, the stagnation enthalpy was set to simulate the Mach 7 flight condition. The stagnation pressure for the HSM was chosen to simulate approximately q=500 psf while the HXEM stagnation pressure was set higher for q=670 psf.

The vitiated air test gas entering the HXEM contains products of methane combustion. The volumetric composition is approximately 9% CO_2, 18% H_2O, and 21% O_2 with a nitrogen balance. Figure 10a shows a point-to-point ratio of HSM pressure along the model centerline with corresponding pressures measured in the HXEM. This figure shows results for HSM run with pure air test gas. The fuel in both cases was 5% by volume of silane in hydrogen and the equivalence ratios were nominally the same. Prior to forming this ratio both data sets were renormalized to matched dynamic pressure. Deviations from unity in this comparison indicate differences in measured pressure distribution between the HSM and HXEM and will be examined for traceability to differences in test technique.

On the forebody, agreement is generally within 20% while larger deviations occur inside the cowl. Some of these differences are attributable to minor differences in shock reflection locations. These are to be expected considering that the test gas in the two tests was not exactly the same. The general trend of the pressure ratio with distance along the engine is to higher values.

Figure 10b is a comparison for a HSM test with a test gas containing 9% CO_2 and 21% O_2 in nitrogen to approximately simulate vitiated air. The mean pressure ratio is approximately 1.2, indicating that the mean pressure level in the two facilities is not quite the same for this comparison. This occurs despite the correction to matched dynamic pressure, indicating further work needs to be done on this correction for HSM when the test gas is not pure air. The overall trend of pressure ratio with distance along the duct is more constant than the previous figure for pure air test gas.

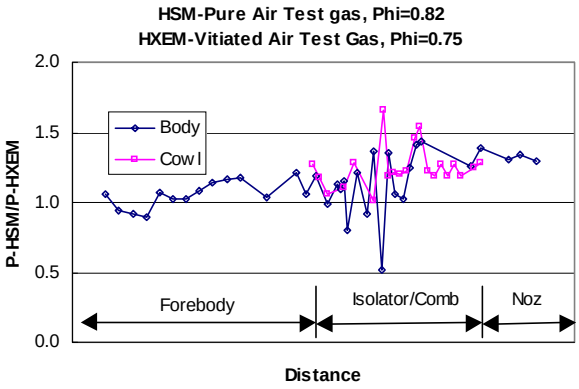

Figure 10(a).- Centerline pressure ratio of HSM with pure air test gas to HXEM with vitiated air

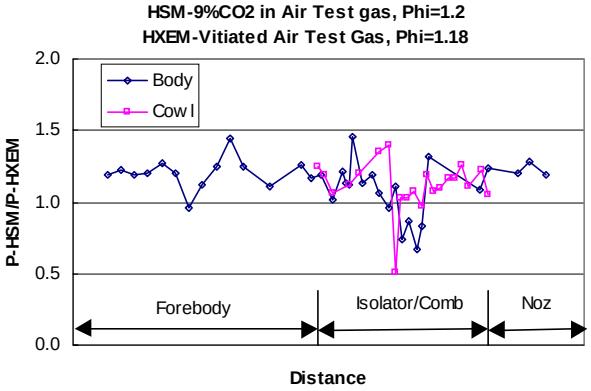

Figure 10(b).- Centerline pressure ratio of HSM with 9% simulated vitiated air to HXEM with vitiated air

CONCLUDING REMARKS

The Mach 10 component of the Hyper-X ground test program will be carried out in the HYPULSE shock tunnel. This facility is now capable of accessing both Mach 7 and 10 flight conditions following upgrades to allow RST operation. The new test cabin can accept large engines for freejet testing and the new nozzle offers up to a 20-inch core diameter, depending on the test condition. The facility has sufficient test time to allow 6-foot or longer models to be tested. A shock tunnel model, designated HSM, has been constructed to replicate a truncated center section of the Hyper-X flowpath. The model is simple in design and allows testing at varying angle of attack at both Mach 7 and Mach 10. The model is thoroughly instrumented with fast response pressure and heat flux gages. Windows in the model sidewall allow flow visualization access to the isolator/combustor and thrust nozzle.

A simulation strategy for Mach 7 and 10 has been developed and testing has begun. The Mach 7

tests provide traceability between HYPULSE data and existing large databases from long-duration test facilities in preparation for Mach 10 flowpath development when the HYPULSE data will stand alone.

Preliminary comparisons of the forebody pressure data with CFD show general agreement indicating that the facility operation is well understood. Pitot surveys of the captured airflow have been obtained and are used, in conjunction with CFD, to define the engine mass capture. Schlieren of the forebody flow agree well with computational density gradient contours. Comparison of the HSM engine pressure data with data from the HXEM model being tested in the vitiated-air, 8-Ft HTT shows reasonable agreement. The results show promise for the confirmation that engine data acquired in the shock tunnel at Mach 10 will lead to a reliable engine design ready for flight test.

ACKNOWLEDGEMENTS

The authors would like to acknowledge the significant contributions to this paper made by Dr. Tom Martin of NYMA, Inc. for his 2D and 3D solutions of the HSM flowfield, and to Mr. Dean Modroukas and Dr. Randy Chue of GASL for their nozzle flow computations.

REFERENCES

1. Orth, R.; and Erdos, J.,: Use of Pulse Facilities for Testing Supersonic Combustion Ramjet (Scramjet) Combustors in Simulated Hypersonic Flight Conditions. Ninth International Symposium on Air Breathing Engines, September 1989.

2. Bakos, R. J.; Tamagno, J.; Rizkalla, O.; Pulsonetti, M. V.; Chinitz, W.; and Erdos, J. I.: Hypersonic Mixing and Combustion Studies in the GASL HYPULSE Facility. Paper 90-2095, AIAA/SAE/ASME/ASEE 26th Joint Propulsion Conference, July 1990.

3. Northam, G. B.; and Anderson, G. Y.: Supersonic Combustion Ramjet Research at Langley. AIAA Paper 86-0159, Jan. 1986.

4. Rogers, R. C.; Capriotti, D. P.; and Guy, R. W.: Experimental Supersonic Combustion Research at NASA Langley. AIAA Paper 98-2506, June, 1998.

5. Rock, K.E. and, Voland, R. T.: NASA's Hyper-X Scramjet Engine Ground Test Program," IS-227, XIV ISABE, September, 1999.

6. McClinton, C. R.; *et. al.*: Wind Tunnel Testing, Flight Scaling and Flight Validation with Hyper-X. AIAA Paper 98-2866, June, 1998.

7. Guy, R. W.; *et. al.:* The NASA Langley Scramjet Test Complex. AIAA Paper 96-3243, July, 1986.

8. Bakos, R. J.; *et. al.*: An Experimental and Computational Study Leading to New Test Capabilities for the HYPULSE Facility with a Detonation Driver. AIAA Paper 96-2193, June 1986.

9. Bakos, R. J.; *et. al.*: Design, Calibration, and Analysis of a Tunnel Mode of Operation for the HYPULSE Facility. AIAA Paper 96-2194, June 1996.

10. Erdos, J. I.; *et. al.*: Dual Mode Shock-Expansion/ Reflected-Shock Tunnel. AIAA Paper 97-0560. Jan. 1997.

11. Modroukas, D.; Betti, A.; Chinitz, W.; and Bakos, R. J.: Design, Fabrication, and Calibration of a Mach 6.5 Hypersonic Shock Tunnel Nozzle for Scramjet Testing Applications. AIAA Paper 98-2496, June 1998.

12. Tsai, C.-Y., Calleja, J.F. and Bakos, R.J., "A Technique For Mixing Measurement In Hypervelocity Pulse Facilities Using Particle Scattering Imagery," AIAA-96-2222, 19th AIAA Advanced Measurement and Ground Testing Technology Conference, June 1996.

13. Lu, F.K. and Liu, X., "Optical Design of Cranz-Schardin Cameras," Optical Engineering, Vol. 36, No.7, pp. 1935-1941, July 1997.

14. Witte, D. W.; and Tatum, K. E.: Computer Code for Determination of Thermally Perfect Gas Properties. NASA TP 3447, Sept. 1994.

NOMENCLATURE

AHSTF		Arc-Heated Scramjet test Facility
BLT	-	Boundary layer trip
CLE	-	Cowl leading edge
FPI	-	Fuel-plume planar imaging
HSM	-	HYPULSE scramjet model
HXEM	-	Hyper-X experimental model
HXRV	-	Hyper-X research vehicle
LHI	-	Laser-holographic interferometry
NASP	-	National Aero Space Plane
PIW	-	Path-integrated water vapor
RST	-	Reflected shock tunnel
SET	-	Shock-expansion tunnel
TPG	-	Thermally perfect gas